

# Journal of Materials Chemistry C

Accepted Manuscript



This is an *Accepted Manuscript*, which has been through the Royal Society of Chemistry peer review process and has been accepted for publication.

*Accepted Manuscripts* are published online shortly after acceptance, before technical editing, formatting and proof reading. Using this free service, authors can make their results available to the community, in citable form, before we publish the edited article. We will replace this *Accepted Manuscript* with the edited and formatted *Advance Article* as soon as it is available.

You can find more information about *Accepted Manuscripts* in the [Information for Authors](#).

Please note that technical editing may introduce minor changes to the text and/or graphics, which may alter content. The journal's standard [Terms & Conditions](#) and the [Ethical guidelines](#) still apply. In no event shall the Royal Society of Chemistry be held responsible for any errors or omissions in this *Accepted Manuscript* or any consequences arising from the use of any information it contains.

# Flexo-electric behavior of bimesogenic liquid crystals in the nematic phase - observation of a new self-assembly pattern at the twist-bend nematic and the nematic interface.

R. Balachandran,<sup>1</sup> V. P. Panov,<sup>1</sup> Yu. P. Panarin,<sup>1,2</sup> J. K. Vij,<sup>1, a)</sup> M. G. Tamba,<sup>3</sup> G. H. Mehl,<sup>3</sup> and J. K. Song<sup>4</sup>

<sup>1)</sup> Department of Electronic and Electrical Engineering, Trinity College, University of Dublin, Dublin 2, Ireland

<sup>2)</sup> School of Electronic and Communication Engineering, DIT, Dublin 8, Ireland

<sup>3)</sup> Department of Chemistry, University of Hull, HU6 7RX, UK

<sup>4)</sup> School of Electronic and Electrical Engineering, SKKU, Suwon, Korea

Flexoelectric properties - the effective flexoelectric coefficient and flexoelectric polarisation are investigated for a bimesogenic liquid crystal CBC11CB with a twist bend nematic phase ( $N_{tb}$ ). Results show that the effective flexoelectric coefficient is at least two times higher than for bimesogens that do not exhibit the  $N_{tb}$  phase. The flexoelectric polarization for the  $N_{tb}$  phase is also two times greater than in its nematic phase. In a temperature gradient cell, we observe surprisingly a new phenomenon, in the bimesogens CBC7CB and CBC9CB and their mixtures with 5CB, of periodic self-assembly in the N phase close to the N -  $N_{tb}$  phase transition temperature. This phenomenon is reminiscent of the self-deformation and spontaneous chirality that appears in the system.

## I. INTRODUCTION

Two mesogens, connected by an odd number of methylene units are shown to exhibit a second nematic phase ( $N_x$ )<sup>1-5</sup> at temperatures below those observed for the characteristic uniaxial nematic (N) phase. This low temperature phase was suggested to be a twist-bend nematic phase ( $N_{tb}$ ) by Cestari *et al*<sup>6</sup>. This was later confirmed to have 8 nm helical pitch simultaneously by two groups using freeze-fracture transmission electron microscopy<sup>7-9</sup>. This is an amazing coincidence with the pitch found from the measurements of the electro-clinic coefficient<sup>10,11</sup>, on assuming the effective flexoelectric coefficient,  $e$ , to be 5 pC/m<sup>10,11</sup>. The complicated internal structure of the phase results in a number of fascinating macroscopic self-assembly properties<sup>12</sup>. When the LC in the  $N_{tb}$  phase is confined to a planar homogeneously rubbed cell of thicknesses ranging from 2 to 10  $\mu\text{m}$ , the cell shows spontaneously formed self-assembled periodic patterns appearing under a polarising optical microscope as uniform stripes parallel to the rubbing direction with a periodicity two times the sample thickness<sup>4</sup>. The phase also exhibits a linear optical response<sup>13</sup> similar to the electroclinic effect with the switching time of the order of a few microseconds. In the achiral materials this is possible due to the formation of macroscopic chiral domains of opposite handedness separated by the domain walls<sup>13</sup>. When a large electric field of a certain frequency range is applied, these domains turn into another type of periodic striped texture, with handedness of the neighboring domains<sup>14</sup> alternating from one to the other. The walls of these domains are normal to the rubbing direction. A range of interesting properties exhibited, so far, by bimesogens in  $N_{tb}$  motivates us to investigate additional macroscopic properties with the final objective

as to how the macroscopic structure evolves from the nanoscale one. In this paper, we investigate the bulk flexoelectric coefficient  $e = |e_1 - e_3|$  in the conventional nematic phase, and the flexoelectric polarization,  $P_f$  in both N and  $N_{tb}$  phases of the bimesogen CBC11CB in order to gain better understanding of the material properties of such systems. In addition, we also report an unusual pre-transitional phenomenon observed in the bimesogens CBC7CB and CBC9CB, and their mixtures with 5CB. The chemical formulae of the liquid crystalline materials studied are given in Fig 1. To the best of our knowledge, such results for this class of materials have not been reported in the literature before. The ultimate question as to what drives this nanoscale helical pitch to the formation of beautiful stripes under cell confinement of thickness of a few  $\mu\text{m}$  needs to be explored. Some of the other intriguing issues that remain to be addressed are (i) how do the competing elastic forces of splay, bend and twist play a role in LC cells under dimensions of a few  $\mu\text{m}$  confinement? (ii) do the bimesogens display large flexoelectric coefficient that drives the electroclinic coefficient? (iii) what happens at the phase transition from a conventional nematic to the  $N_{tb}$  phase?

## II. RESULTS AND DISCUSSION

The flexoelectric polarization arising from a coupling between the elastic deformations and the electric polarization is expressed in terms of the splay and bend flexoelectric coefficients by Meyer<sup>15</sup> as follows:

$$P_f = e_1 \mathbf{n}(\nabla \cdot \mathbf{n}) - e_3 [\mathbf{n} \times (\nabla \times \mathbf{n})] \quad (1)$$

In equation (1),  $e_1$  and  $e_3$  are the flexoelectric coefficients that correspond to the splay and bend deformations, respectively. Flexoelectric coefficients in bimesogens, measured using indirect methods, are found to

<sup>a)</sup>To whom correspondence be addressed: Email: jvij@tcd.ie

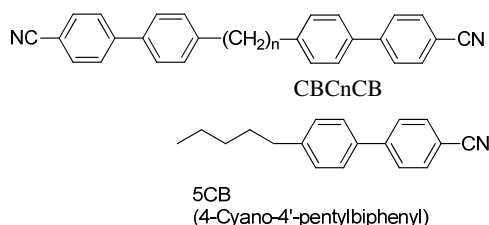


FIG. 1. Chemical formula of liquid crystalline material studied for pyroelectric and flexoelectric measurements: CBC11CB. Mixtures of CBC9CB and CBC7CB were prepared for up to 42 % of 5CB in order to investigate the pre-transitional effects. The transition temperatures for each mixture are different.  $n = 7$ : CBC7CB + 0% 5CB [ $N_{tb}$  103 N 116 Iso], + 20% 5CB [ $N_{tb}$  72 N 92 Iso], + 30% 5CB [ $N_{tb}$  53 N 80 Iso], + 34% 5CB [ $N_{tb}$  51 N 75 Iso], + 42% 5CB [ $N_{tb}$  42 N 65 Iso]; ( $n = 9$ : CBC9CB + 0% 5CB [ $N_{tb}$  109 N 124 Iso], + 20% 5CB [ $N_{tb}$  78 N 102 Iso], + 30% 5CB [ $N_{tb}$  65 N 93 Iso], + 34% 5CB [ $N_{tb}$  56 N 83 Iso], + 42% [ $N_{tb}$  45 N 74 Iso]; CBC11CB, [ $N_{tb}$  108.7 N 125.3 Iso]. Values inside the square brackets in all cases indicate the transition temperatures in  $^{\circ}\text{C}$ .

be larger than conventional calamitics<sup>16,17</sup>. The indirect/converse methodology for obtaining the flexoelectric coefficient is based on the gradient stress produced by the external electric field through exploiting the uniform lying helical (ULH) geometry obtained in a cholesteric nematic phase<sup>18</sup>. The latter is obtained by adding a small concentration of a large helical twisting power dopant to the liquid crystal sample. Flexoelectricity in such systems manifests itself in terms of the rotation of optic axis on the application of an electric field perpendicular to the helical axis<sup>18</sup>. For small  $E$ , tilt angle is linearly related to the applied electric field by

$$\tan(\phi) = \frac{e'p}{2\pi K} E \quad (2)$$

$e'$  and  $K$  are the effective flexoelectric and the elastic coefficients defined as:  $e' = \frac{|e_1 - e_3|}{2}$ ,  $K = \frac{K_{11} + K_{33}}{2}$ ,  $p$  is the helicoidal pitch of the ULH. Hence, one can calculate the effective flexoelectric coefficient if the pitch, splay and bend elastic constants are known.

Planar aligned cells are fabricated using indium tin oxide (ITO) glass plates coated with polymer alignment layer RN1175 (Japan) and cured at  $250^{\circ}\text{C}$  for  $\sim 1.5$  hours. The glass plates are assembled together with anti-parallel rubbing directions on the top and bottom substrates. The typical thickness of the cell used for the flexo-electric experiment is  $5\text{-}6 \mu\text{m}$ . The cholesteric mixture is prepared by adding a small concentration ( $\sim 3\%$ ) of a large helical twisting power chiral agent R5011 (right handed dopant supplied by Merck Korea, helical twisting power (HTP)  $100 \mu\text{m}^{-1}$ ) to the original sample. The low concentration of the additive ensures that the properties of the host sample are not modified by the chiral dopant. The texture in the ordinary nematic phase of the chiral mixture is typical of a classical cholesteric liquid

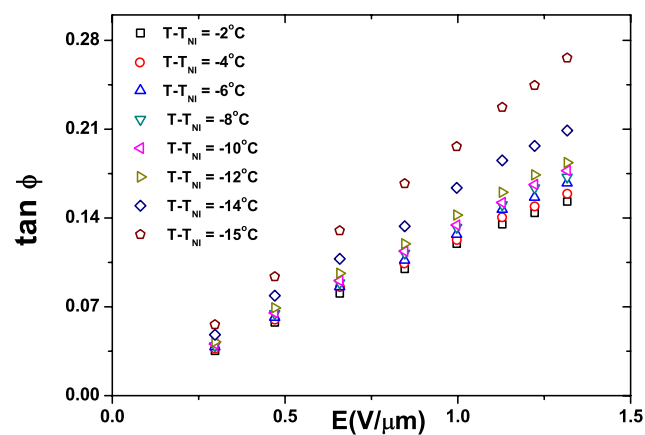


FIG. 2. (color online) Tangent of the tilt angle is plotted as a function of the applied field for a range of reduced temperatures.

crystal in a planar aligned cell. Hence the technique of obtaining  $|e_1 - e_3|$  using a ULH is valid for the higher temperature  $N^*$  phase. However in the lower temperature  $N_{tb}$  phase, rope-like textures were observed (see Supplementary Information); these are rather different from the higher temperature  $N^*$  phase. This implies that ULH technique cannot be used to evaluate  $|e_1 - e_3|$  in this phase due to its non-uniform structure. The optical pitch in the  $N^*$  phase is obtained by measuring the wavelength of selective reflection of light incident normally on a planar cell by a UV/VIS Spectrometer (Avaspec-2048). The pitch is found to be nearly invariant for higher temperatures, however it increases significantly from  $\sim 420$  to  $535$  nm at temperatures closer to the  $N - N_{tb}$  phase transition temperature as shown in Fig. 3. The divergence of the pitch in the  $N^*$  phase on cooling is presumably an intrinsic property of the chiral dopant R5011, as the same additive in another (bent-core) system produced a pitch that varied significantly with reduced temperature<sup>19</sup>.

The uniform lying helical structure (ULH) is formed only under special conditions<sup>18</sup> as the minimum free energy of a chiral nematic leads to a Grandjean configuration where the helical axis lies perpendicular to the substrates. In order to induce ULH, the cell is cooled from the isotropic to the cholesteric nematic phase at a rate of  $0.1^{\circ}\text{C}/\text{min}$  under the influence of a moderate electric field ( $E \sim 2\text{V}/\mu\text{m}$ ,  $f = 100$  Hz) applied across the cell. Once the ULH evidenced by its characteristic texture is obtained, the tilt angle is calculated using the procedure given before<sup>20</sup>. The applied fields are lower than required for complete helical unwinding in order to satisfy the conditions used in deriving Eqn(2). Data for the elastic constants and the dielectric anisotropy for CBC11CB are taken from our results on the same material<sup>21</sup>. A linear relationship between  $\tan \phi$  and  $E$  (Fig. 2) is obtained for several reduced temperatures. As seen from this figure, flexoelectrically induced rotation angle  $\phi$  shows noticeable increase at temperatures closer to the  $N\text{-}N_{tb}$  transition temperature. The growth in the rotation angle is

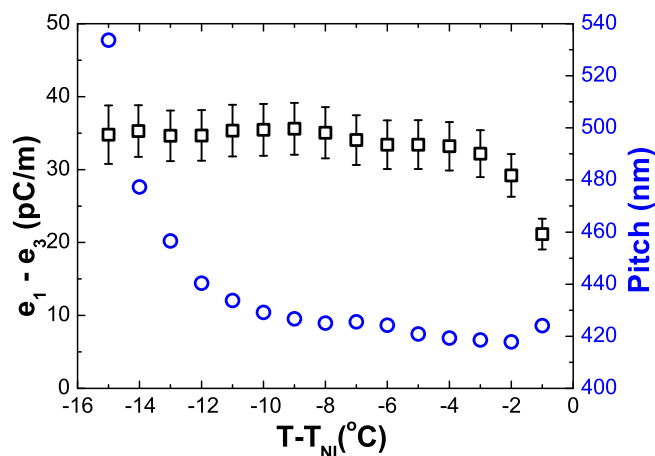


FIG. 3. (color online) The effective flexoelectric coefficient (black squares), multiplied by two plotted as a function of reduced temperature. Helical pitch values used for calculation (blue circles). Planar cell of thickness  $5.5 \mu\text{m}$  filled with CBC11CB + 3% R5011 mixture.).

possibly due to increase in the helical pitch as temperature decreases;  $p$  is directly proportional to  $\tan \phi$  (see Eqn. 2).

The convention introduced by Coles *et. al.*<sup>22</sup> about the sign of  $(e_1 - e_3)$  when applied, sets its sign to be positive. It is noted that  $|e_1 - e_3|$  increases from 21 pC/m at  $T - T_{NI} = -1^\circ\text{C}$  to 35 pC/m for  $T - T_{NI} = -15^\circ\text{C}$ . It would have been interesting to obtain data at temperatures closer to the N-  $N_{tb}$  phase transition. However, the resulting flexo-electric signal degrades at these temperatures significantly and the reliable flexoelectric coefficient data close to the N- $N_{tb}$  phase transition could not be obtained.

The effective value of the flexoelectric coefficient is higher by a factor 1.5 to 2.0 than the highest values determined for the bent core systems C4 to C7 recently studied by us<sup>21</sup>. These are also greater by a factor of 2 than an odd ether-linked bimesogen<sup>16</sup> that do not exhibit the  $N_{tb}$  phase. Values are rather similar to those measured for an ester-linked fluorine substituted asymmetric bimesogen at lower temperatures<sup>23</sup>. Note that Atkinson *et. al.*<sup>16,23</sup> plot  $|e_1 - e_3|/2$  instead of  $|e_1 - e_3|$  being plotted here in Fig. 3. Due to the average bent-shape of the molecules, the bend flexoelectric coefficient is expected to be greater in odd bimesogens. This possibly results in higher values of  $|e_1 - e_3|$  in CBC11CB when compared to conventional calamitics. The difference in the value of the effective flexoelectric coefficient from the other bimesogenic systems at comparable temperatures may arise from the different electric structure of the dimers, as well as their geometry and flexibility<sup>26</sup>.

Figure 4 gives the temperature dependence of the pyroelectric signal. The flexo-electric polarization  $P_f$  is obtained by integrating the pyroelectric signal measured from a  $7.7 \mu\text{m}$  hybrid cell filled with CBC11CB. The

alignment on one of the substrates was planar and on the other was homeotropic. The pyroelectric coefficient is a property of the material itself hence the cell thickness does not affect its value as such, but it may influence the experimental errors. The cell parameters used in this experiment produced a good signal to noise ratio and a reasonable alignment of the material. The peaks that appear at  $T = 126.6^\circ\text{C}$  and  $107^\circ\text{C}$  (on cooling the liquid crystal) refer to the Iso-N and N- $N_{tb}$  phase transitions, respectively. The pyroelectric signal in the isotropic phase is not zero and differs in phase presumably due to the presence of a strong surface polarization in the sample<sup>24</sup>. This phasor vector was subtracted when calculating  $P_f$ . The measurements were made in the absence of an electric field, hence the potential effects such as the ionic screening and coupling of dielectric anisotropy to the electric field were neglected. The absolute values of  $P_f$  can be calculated by determining the temperature increment i.e. the time rate of change of temperature of the sample as a result of heating from the light source. Alternatively the system can be calibrated by determining the scaling factor required to obtain the absolute value of the pyroelectric coefficient. The absolute calibration of the amplitude of the pyroelectric response, necessary for determining the pyroelectric coefficient,  $\gamma$ , was carried out by using the spontaneous polarization  $P_S$  value of a well known ferroelectric liquid crystal 12OF1M7. This was measured using the standard repolarization current technique<sup>25</sup>. The pyroelectric signal for 12OF1M7 was recorded using the same measurement conditions as for CBC11CB. The integrated pyroelectric signal of 12OF1M7 was then scaled to  $P_S$  value obtained using field reversal method. This yielded the necessary calibration factor. Fig. 4 shows the magnitude of  $|P_f|$  determined for CBC11CB. Its value increases on transition from the isotropic phase and is seen to grow marginally from 0.08 to 0.10  $\text{nC cm}^{-2}$  in the nematic phase, as the temperature is further reduced in the  $N$  phase. It is observed to increase steadily on cooling at the transition into the  $N_{tb}$  phase. It reaches almost 0.17  $\text{nC cm}^{-2}$  at the lowest temperatures for which measurements were carried out. Results show for the first time that  $N_{tb}$  phase has a larger flexoelectric polarization by a factor of almost 2, compared to the classical nematic phase. This possibly is the source of a large electroclinic effect observed in this phase<sup>10,13</sup>. In the literature, flexoelectric polarization has been determined in the nematic phase of a classical calamatic system 5CB<sup>27</sup>. This was found to be 0.04  $\text{nC cm}^{-2}$  at  $25^\circ\text{C}$  and its value within the experimental error is being confirmed using our experimental set-up. Furthermore these result on CBC11CB may also indicate that splay deformations may significantly influence the macroscopic effects exhibited by twist-bend nematic phase especially close to the transition temperature. This implies that as the macroscopic structure evolves from the nanostructure, splay deformations can also have a role especially in exhibiting macroscopic effects.

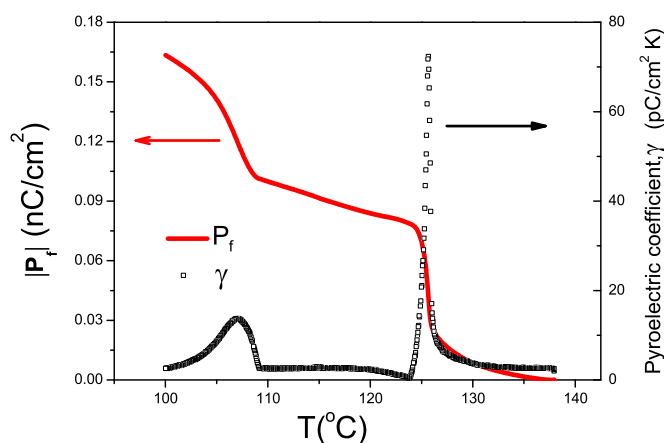


FIG. 4. (color online) Temperature dependence of the pyroelectric signal and flexoelectric polarization of CBC11CB.

We observe unusual effects in bimesogens CBC7CB and CBC9CB and their mixtures with the monomer (5CB) in a temperature gradient cell. In a narrow temperature range close to the  $N$ - $N_{tb}$  phase transition, a new type of stripe pattern is observed under a polarizing microscope (Fig. 5). This is accompanied by the appearance of rainbow colors and is present only in a narrow temperature range close to the  $N$  and  $N_{tb}$  phase transition temperature. This effect is not seen under fast heating or cooling and observed in cells with a thickness  $> 8\mu\text{m}$ , which indicates that this effect is not caused by the cell surfaces. The planar cells of thickness 15 and  $25\mu\text{m}$  are used to demonstrate this phenomenon.

TABLE I. The periodicity of the striped patterns given in (**bold**) and the temperature ranges associated with “rainbow like colors” for the various mixtures and the cell gaps.

% of 5CB	0%	20%	30%	34%	42%
CB-C7-CB 15 $\mu\text{m}$	0.08 $^{\circ}\text{C}$ no	0.03 $^{\circ}\text{C}$ <b>1.93<math>\mu\text{m}</math></b>	0.06 $^{\circ}\text{C}$ <b>2.74<math>\mu\text{m}</math></b>	0.06 $^{\circ}\text{C}$ no	0.03 $^{\circ}\text{C}$ no
CB-C7-CB 25 $\mu\text{m}$	0.16 $^{\circ}\text{C}$ no	0.08 $^{\circ}\text{C}$ <b>2.2<math>\mu\text{m}</math></b>	0.25 $^{\circ}\text{C}$ <b>2.94<math>\mu\text{m}</math></b>	0.12 $^{\circ}\text{C}$ no	0.06 $^{\circ}\text{C}$ no
CB-C9-CB 15 $\mu\text{m}$	0.08 $^{\circ}\text{C}$ no	0.1 $^{\circ}\text{C}$ <b>2.94<math>\mu\text{m}</math></b>	0.08 $^{\circ}\text{C}$ no	0.03 $^{\circ}\text{C}$ no	0.0 $^{\circ}\text{C}$ no
CB-C9-CB 25 $\mu\text{m}$	0.1 $^{\circ}\text{C}$ no	0.2 $^{\circ}\text{C}$ <b>3.27<math>\mu\text{m}</math></b>	0.13 $^{\circ}\text{C}$ no	0.08 $^{\circ}\text{C}$ no	0.04 $^{\circ}\text{C}$ no

The periodicity of the new stripes varies as a function of both concentration and the cell gap. In the pure materials, the stripes are not readily visible but these can be detected as the concentration of 5CB is increased. However, beyond a certain concentration of 5CB, the phenomenon disappears completely. The periodicity of the stripes together with a temperature range of the rainbow colors for the various cell thicknesses and concentrations have been studied for both sets of bimesogens CBC7CB and CBC9CB, and their mixtures with 5CB. The temperature range of this transition phenomena is estimated

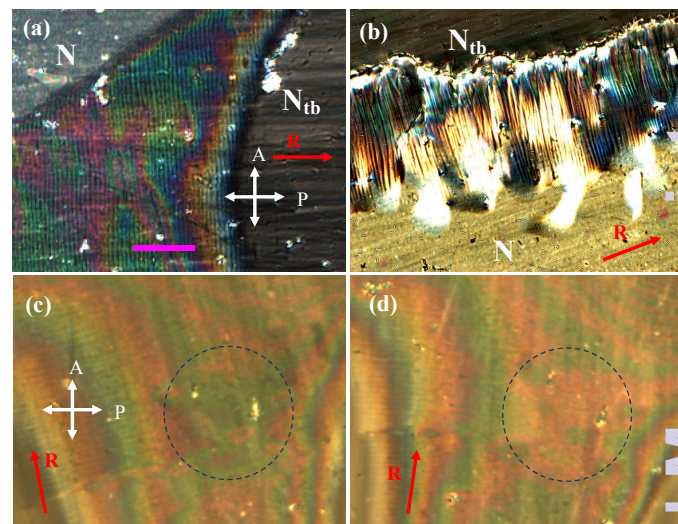


FIG. 5. (color online) POM textures obtained in a  $25\mu\text{m}$  cell filled with the sample (CB-C7-CB + 30% 5CB) when viewed under cross-polarizers on slowly cooling the cell from the nematic phase. (a) the observed striped region between the  $N$  and  $N_{tb}$  phase using a 10X lens magnification observed at a temperature  $52.75^{\circ}\text{C}$  (length of the magenta bar is  $24\mu\text{m}$ ). The stripes are uniform and have a periodicity of  $2.94\mu\text{m}$ . The red arrow depicts the rubbing direction. (b) the effect of an electric field (10 V, frequency 10 kHz, temperature  $52.82^{\circ}\text{C}$ ) applied across the cell in this narrow temperature range. With the field applied, the stripes are not uniform anymore but the region is distinct from the other two phases, with a wider, non-uniform striped pattern.  $N_{tb}$  is still planar, while nematic is almost homeotropic at this field. In (c) and (d) colors obtained are compared when the rubbing direction rotated left (c) and right (d) from the axis of the crossed polarizers. The circle diameter is  $80\mu\text{m}$ .

to be less than  $0.1^{\circ}\text{C}$  and appears to be primarily a function of the temperature gradient in the particular experiment, but also as a function of cell gap and to a certain extent depends on concentration of 5CB in the mixture. When a second heater was introduced on top of the sample cell, the temperature range of the observed phenomena decreases significantly and in some cases vanishes altogether, highlighting its association with the temperature gradient across the cell. The periodicity of the striped pattern, however, remains unaffected, suggesting that the rainbow colors are related to the temperature gradient, while the stripes are independent of it. Table I shows temperature ranges found in different cells and mixtures under similar temperature gradient conditions in the absence of the second heater. To explain the observed phenomenon, we refer to the geometry shown in fig 6. The rainbow colors and their behavior as a function of the cell gap can then be explained by the interference on the wedge made with the materials of different birefringence and refractive indices (i.e.  $N$  and  $N_{tb}$  phases). However, the interchange of the colors on rotating the sample between the crossed polarizers (Figure

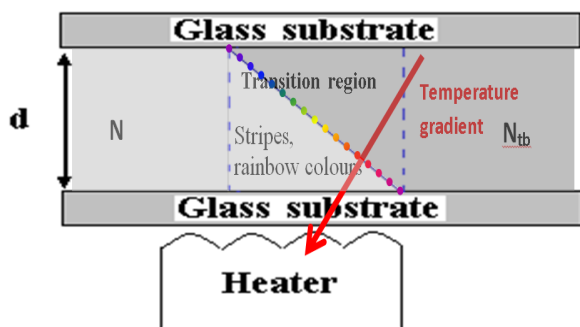


FIG. 6. (color online) The temperature gradient in a heating stage causes the interface between  $N_{tb}$  and nematic phases to form wedge-like confinement for each phase.

5(c, d)) implies that not only the birefringence, but also an optical rotation is involved. This indicates presence of self-deformation and spontaneous chirality in the system. The fluctuations seen in the transition region appear to originate from a thin layer of the nematic phase present at the bottom (warmer) glass substrate, while the  $N_{tb}$  phase is present closer to the top substrate (colder surface)[Fig. 6]. The periodic pattern can be attributed to the interface present between the two phases. The electric field switches the nematic phase by Fredericksz transition whereas the applied field causes the stripes to become non-uniform and wider, seen in Fig. 5b. It is likely that the presence of a thin film of aligned nematic phase improves the visibility of an intrinsic pattern of the  $N_{tb}$  phase. We however note that the observed phenomenon does not arise from the Grandjean texture, likely to be seen on confining a material with a short helical pitch in a wedge geometry. In our case the stripes appear normal to the rubbing direction and these are independent of the magnitude and direction of the temperature gradient (visualized by the rainbow colors), i.e. these are not caused by the wedge shape (Fig. 6) of the  $N_{tb}$  (or N) sections of the sample.

### III. CONCLUSION

We have obtained the difference in the bulk flexoelectric coefficient,  $|e_1 - e_3|$  in CBC11CB in the N phase for a bimesogenic system which exhibits the  $N_{tb}$  phase below the ordinary nematic phase by studying the converse flexo-electric effect in a ULH system. The optical pitch is nearly temperature independent at higher temperatures, but increases steadily at lower temperatures, closer to the  $N_{tb}$  phase.  $\tan \phi$  follows a linear relationship at lower fields in accordance with Eqn(2). The tilt angle at temperatures close to the  $N_{tb}$  phase was seen to increase substantially in comparison to the higher temperatures, where  $\phi$  was observed to be nearly independent of it. The value of  $|e_1 - e_3|$  was seen to be nearly independent of temperature after an initial increase below the transition from the isotropic phase with

values ranging from  $\sim 21$ -35 pC/m. The  $e/K$  ratio in this compound is almost greater by a factor of 1.7 and  $|e_1 - e_3|$  is almost twice higher for CBC11CB than reported for the bimesogen studied in ref.<sup>16</sup> and similar to that estimated for ester-linked fluorine substituted asymmetric bimesogens<sup>23</sup>. These bimesogens show relatively large flexoelectric polarization which undoubtedly gives rise to the large electroclinic effect already reported by the authors<sup>13</sup>. In some of these bimesogens and their mixtures with 5CB, we have observed micrometer scale stripes at the  $N$ - $N_{tb}$  transition temperature, indicating yet another surprising chiral self-assembly phenomenon observed in this class of materials. The change in the elastic constants with temperature closer to  $N$ - $N_{tb}$  transition may be one of the reasons for such observations.

One of the authors (RB) thanks Irish Research Council for the award of a research studentship. Cooperation with Jan-Kung Song evolved as two of the authors (V. Panov and JKV) spent parts of the academic year 2013-14 in SKKU, Korea supported in the latter case by the WCU program of the National Research Foundation of Korea funded by Ministry of Education, Science and Technology.

### IV. REFERENCES

- <sup>1</sup>C. T. Imrie and P. A. Henderson, *Chem. Soc. Rev.* 2007, **36**, 2096-2124.
- <sup>2</sup>P. A. Henderson and C.T. Imrie, *Chem. Soc. Rev.* 2011, **38**, 1407-1414.
- <sup>3</sup>D. A. Dunmur, G. R. Luckhurst, M. R. de la Fuente, S. Diez, and M. A. Perez Jubindo, *J. Chem. Phys.*, 2001, **115**, 8681-8691.
- <sup>4</sup>V. P. Panov, M. Nagaraj, J. K. Vij, Y. P. Panarin, A. Kohlmeier, M. G. Tamba, R. A. Lewis and G. H. Mehl, *Phys. Rev. Lett.*, 2010, **105**, 167801.
- <sup>5</sup>R. J. Mandle, E. J. Davis, C. T. Archbold, S. J. Cowling, and J. W. Goodby, *J. Mater. Chem. C* 2014, **2**, 556-566.
- <sup>6</sup>M. Cestari, S. Diez-Berart, D. A. Dunmur, A. Ferrarini, M. R. de la Fuente, D. J. B. Jackson, D. O. Lopez, G. R. Luckhurst, M. A. Perez-Jubindo, R. M. Richardson, J. Salud, B. A. Timimi and H. Zimmermann, *Phys. Rev. E*, 2011, **84**, 031704.
- <sup>7</sup>D. Chen, J. H. Porada, J. B. Hooper, A. Klittnick, Y. Shen, M. R. Tuchband, E. Korblova, D. Bedrov, D. M. Walba, M. A. Glaser, J. E. MacLennan, and N. A. Clark, 2013, *PNAS* **110**, 15931.
- <sup>8</sup>V. Borshch, Y-K Kim, J. Xiang, M. Gao, A. Jakli, V. P. Panov, J. K. Vij, C. T. Imrie, M.G. Tamba, G. H. Mehl and O. D. Lavrentovich, *Nature Communications*, 2013, **4**, DOI:10.1038/ncomms3635.
- <sup>9</sup>C. Greco, G.R. Luckhurst and A. Ferrarini, *Phys. Chem. Chem. Phys.*, 2013, **15**, 14961-14965.
- <sup>10</sup>C. Meyer, G.R. Luckhurst and I. Dozov, *Phys. Rev. Lett.*, 2013 **111**, 067801.
- <sup>11</sup>I. Dozov, *EPL*, 2001, **56**, 247-253.
- <sup>12</sup>V. P. Panov, J. K. Vij, R. Balachandran, V. Borshch, O. D. Lavrentovich, M. G. Tamba, and G. H. Mehl, *Proc. SPIE, Liquid Crystals XV11*, 2013, **8828**, 88280X, doi: 10.1117/12.2024470.
- <sup>13</sup>V. P. Panov, R. Balachandran, M. Nagaraj, J. K. Vij, M. G. Tamba, A. Kohlmeier, and G. H. Mehl, *Appl. Phys. Lett.*, 2011, **99**, 261903.
- <sup>14</sup>V. P. Panov, R. Balachandran, J. K. Vij, M. G. Tamba, A. Kohlmeier, and G. H. Mehl, *Appl. Phys. Lett.*, 2012, **101**, 234106.
- <sup>15</sup>R. B. Meyer, *Phys. Rev. Lett.*, 1969, **22**, 918-921.

- <sup>16</sup>K. L. Atkinson, S. M. Morris, F. Castles, M. M. Qasim, D. J. Gardiner, and H. J. Coles, *Phys. Rev. E* **85**, 2012, 012701.
- <sup>17</sup>H. J. Coles, M. J. Clarke, S. M. Morris, B. J. Broughton, and A. E. Blatch, *J. Appl. Phys.*, 2006, **99**, 034104.
- <sup>18</sup>J. S. Patel and R. B. Meyer, 1987, *Phys. Rev. Lett.* **58**, 1538-1540.
- <sup>19</sup>P. S. Salter, C. Tschierske, S. H. Elston and E. P. Raynes, 2011 *Phys. Rev. E* **84**, 031708.
- <sup>20</sup>R. Balachandran, V. P. Panov, J. K. Vij, A. Lehmann, and C. Tschierske, *Phys. Rev. E*, 2013 **88**, 032503.
- <sup>21</sup>R. Balachandran, V. P. Panov, J. K. Vij, A. Kocot, M. G. Tamba, A. Kohlmeier and G. H. Mehl, *Liq. Cryst.*, 2013, **40**, 681-688.
- <sup>22</sup>F. Castles, S. C. Green, D. J. Gardiner, S. M. Morris and H. J. Coles, 2012, *AIP Advances*, **2**, 022137.
- <sup>23</sup>K. L. Atkinson, S. M. Morris, M. M. Qasim, F. Castles, D. J. Gardiner, P. J. W. Hands, S. S. Choi, W.-S Kim and H. J. Coles, *Phys. Chem. Chem. Phys.*, 2012, **14**, 16377-163855.
- <sup>24</sup>N. M. Shtykov, M. I. Barnik, and V. P. Panov, *JETP*, 2000 **91**, 126-129.
- <sup>25</sup>Yu. P. Panarin, O. E. Kalinovskaya, J. K. Vij, J. W. Goodby, *Phys. Rev. E*, 1997, **55**, 4345-4353.
- <sup>26</sup>M. Cestari, E. Frezza, A. Ferrarni and G. R. Luckhurst, *J. Mater. Chem.*, 2011, **21**, 12303-12308.
- <sup>27</sup>L. M. Blinov, M. I. Barnik, M. Ozaki, N. M. Shtykov, and K. Yoshino, *Phys. Rev. E*, 2000, **62**, 8091-8099.

Flexoelectricity in bimesogenic liquid crystal exhibiting  $N_{tb}$  phase is higher than in bimesogens without it.  $N$ - $N_{tb}$  interface shows periodic self-assembly pattern.

